NUCLEAR MAGNETIC RESONANCE IN THE ANALYSIS OF DAIRY PRODUCTS

Elvino Brosio and Renato Barbieri

Department of Chemistry
University of Rome "La Sapienza"
Rome, Italy

CONTENTS

Page

Summary 273
Introduction 274
Low-resolution NMR in the study of milk and milk derivatives 275
Diffusion measurements 279
High-resolution NMR of cheese 287
High-resolution NMR of milk 289
Conclusions 290
References 290

SUMMARY

Nuclear Magnetic Resonance (NMR) is a non-invasive, multiparametric technique particularly suitable for the study of heterogeneous systems. In this paper some applications to the study of milk and milk derivatives are reviewed and discussed.

Low resolution ^1H NMR is primarily involved in spin-spin relaxation time and self-diffusion coefficient measurements of water and fat molecules in dairy products. From these parameters, information about molecule dynamics, chemical exchange kinetics and sample morphologies can be obtained. In addition, the time-dependence monitoring of such parameters

during processes such as renneting or cheese ripening can be used for *in situ* determination of the endpoint of the process itself.

Solid-state high resolution ^{13}C NMR spectra can be used to get information on both chemical composition and structure of the solid matrix of different types of cheese.

Finally, *^{31}P high resolution NMR* allows investigation of the chemical composition of the liquid phase of milk and milk derivatives with respect to phosphorus-containing metabolites.

INTRODUCTION

Nuclear Magnetic Resonance (NMR) is a powerful technique for determining the chemical structure, chemical composition and physical properties of different components in a sample. The possibility of using a non-invasive technique to obtain information on the chemical and physical structure of complex, heterogeneous materials makes NMR particularly suitable for the study of food products, in which the textural properties are dependent on physical state, microdynamics and interactions of the different components.

The only problem with NMR is its intrinsic low sensitivity. For this reason NMR is used to obtain information on the most abundant components of foods – water, lipids, proteins and carbohydrates – while it is not well suited for the study of components present at only trace level, such as colorants and flavours. However, other characteristics of NMR (it is completely non-invasive, it is not time consuming, it does not need any pretreatment of the sample) and the wealth of detailed information that can be obtained, largely compensate for the low sensitivity of the technique.

The inherent insensitivity of NMR is the reason why ^{1}H NMR is used for the analysis of food systems, even if in some cases less sensitive nuclei like ^{13}C, ^{31}P, ^{17}O and ^{23}Na are used.

Depending on the different experimental equipment employed we distinguish a variety of NMR techniques: *low-resolution NMR, high-resolution NMR, solid-state high-resolution NMR* and *NMR imaging.*

High-resolution NMR is the area of NMR with which chemists are most familiar and is concerned with the elucidation of the chemical structure of molecules in solution, so that its use in the study of food products is

somewhat limited by the need to have the component to be studied in solution.

Low-resolution NMR is concerned with the quantitative determination of the different components in a sample by the analysis of the amplitudes and the decay rates of the NMR signal and is the technique that has most extensively been used for food analysis /1/. This is mainly due to the possibility of studying the properties of water – a very abundant probe, whose amount, dynamic state and interaction with solid matrixes affect many of the properties of food products. Furthermore, it has to be pointed out that, once developed, the standard protocols based on rapid measurements obtained by low-cost NMR instruments can be easily transferred to on-line quality control applications.

The use of *solid-state high-resolution NMR* to study dairy products is in its infancy and is concerned with the elucidation of chemical structure and conformation of solid components (proteins and carbohydrates) in the sample.

Finally, *NMR Imaging* enables one to describe the internal morphology of the materials to be investigated with an on-plane resolution of up to 10 μm and slice thickness of about 1 mm. Its potential lies in the possibility of obtaining resolved spectra from different regions within the image and of monitoring dynamic events, such as the migration of water, during the processing, ripening and storage of cheese.

In this paper some examples of the use of different NMR techniques in the study of milk derivatives are reported.

LOW RESOLUTION NMR IN THE STUDY OF MILK AND MILK DERIVATIVES

T_2 measurements

Water is the most abundant component in milk (~85%) and it is extensively present in all types of cheese (from 25 to 75%). It plays an essential role in determining the structure of proteins, polysaccharides and lipid aggregates, influencing the texture and stability of the final product. This is why it is important to study the dynamic properties of water and the interactions with other components in the system.

NMR relaxation and diffusion measurements have been shown to give detailed information on the state of water, to be a sensitive probe in the study of structure changes associated with protein and/or lipid components and to provide insight into the dimension and geometry of diffusive domains.

Both longitudinal and transverse relaxation processes are related to different aspects of the motion and interaction of water molecules but, although measurements of T_1 are more reliable than T_2 measurements, the transverse relaxation time is generally used to investigate the state of water in heterogeneous systems. This is because, for proton transverse relaxation, the contribution of cross relaxation between water molecules and macromolecules protons can be neglected, and because slowly fluctuating components of local fields (deriving from low frequency molecular motions) influence T_2 while not affecting T_1.

Water transverse relaxation time can be accurately and rapidly measured by the Carr-Purcell-Meiboom-Gill (CPMG) sequence /2/, but care must be taken in interpreting the experimental results.

The traditional description of water molecules, as being in a bound or free state /3,4/ when multiexponential relaxation is observed, now appears an oversimplification. Indeed, it has been shown /5,6/ that diffusive exchange of water between regions with different relaxation rate or resonance frequency can account for a number of experimental observations without recourse to the concepts of free and bound water. The relaxation behaviour is in fact greatly influenced by the dimensions of diffusive domains. A single exponential is observed if the scale of heterogeneity is small, and the nuclear spins experience all environments in a time that is short compared with the relaxation times and the inverse of Larmor frequency differences. If the scale of heterogeneity is large, diffusional averaging is incomplete and multiexponential relaxation is observed. Furthermore, the higher transverse relaxation rate with respect to that of pure water, generally observed for water in heterogeneous systems, can be explained in terms of chemical exchange between water protons and exchangeable hydrogens (-OH, -NH, -SH) of the macromolecular component in the system.

According to a general model that accounts for chemical exchange, the observed transverse relaxation rate of water is given by:

$$\frac{1}{T_2} = \frac{P_f}{T_{2f}} + \frac{P_b}{T_{2b}} + \frac{P_e}{(T_{2e} + k_e^{-1})} \qquad (1)$$

where T_{2f}, T_{2b} and T_{2e} are the relaxation times of protons of *free water* molecules, of water molecules directly interacting with proteins (the so-called *bound water*) and of exchangeable protons from protein side chains or carbohydrates, respectively; P_f, P_b and P_e are the relative populations of the different types of protons; and k_e^{-1} is the mean life time of exchangeable protons on proteins or carbohydrates. This equation is valid if NMR experiments are performed at low magnetic fields, where the chemical shift differences between exchangeable and water protons are small, and at high fields in the short pulse spacing limit, if there is a rapid diffusive exchange between free and bound water protons, that is $k_b^{-1} \ll T_{2b}$, where k_b^{-1} is the lifetime of water in the bound state.

K_e, the value of the kinetic constant for the exchange rate, and P_e, the fraction of macromolecule protons involved in the exchange process, can be obtained from the dependence of relaxation rate on pulse spacing in the CPMG experiment at high field /5/. The latter quantity can give useful information on structure variation of the macromolecular component.

In any case relaxation times can be used as empirical parameters to monitor any transformation of the system. For example, proton transverse relaxation time measurements have been used to investigate whey protein thermal denaturation /7/, by measuring changes in water T_2 values following a denaturating treatment. For homogeneous aqueous solutions of whey protein concentrate, β-lactoglobulin, α-lactalbumin, bovine serum albumin and immunoglobulins, the curves relating transverse relaxation rates, measured from the temperature T=20°C, to the heating temperature of the samples, were similar: no change in relaxation rate was observed after heating whey protein concentration, β-lactoglobulin, bovine serum albumin solutions up to 55060°C, and immunoglobulin and α-lactalbumin samples up to 70°C and 80°C, respectively. Then a sharp and significant increase of relaxation rate (3-4 times), proportional to protein concentration, resulted from thermal treatment and no further change was observed for heating at higher temperatures.

The increase of T_2 relaxation rate following thermal treatments of protein solutions was interpreted as an effect of the mobility decrease of the water fraction interacting with proteins (a decrease of T_{2b} from 11 to 4 ms was measured). The thermal treatment in fact causes protein unfolding, usually followed by protein aggregation and possibly gelation. As variations in relaxation parameters are also observed when gelation does not occur

(e.g. samples with low protein concentrations), the increase in water relaxation rate following protein unfolding is probably due to a higher contribution of chemical exchange on the T_2 value, due to an increased accessibility of protein protons to water interaction (increase of P_e in eq. 1).

In any case, quantitative variations in water transverse relaxation rate occurring after heating of whey protein solutions can be used to measure the degree of protein denaturation.

Due to the importance of acidification of milk in different manufacturing processes like yogurt and cheese, transverse relaxation time has also been measured to investigate the effect of pH on skim-milk /8,9/. A very strong effect has been found at every measuring temperature; a well defined maximum in T_2 values is in fact observed at pH values between 5.0 and 5.2. As T_2 values for the milk ultrafiltrates are not influenced by pH, the maximum found in T_2 values has been ascribed to a change in the structure of the casein particles upon acidification, which causes an increase in protein hydratation. The low T_2 of skim-milk and of sodium caseinate dispersion at low pH thus implies that water inside casein particles is to some extent immobilized. An analysis of dispersion CPMG curves indicates that both the proton exchange mechanism and *bound water* contribute to the proton relaxation rate in skim-milk. However, ^{17}O relaxation time measurements /9/, which are not complicated by the exchange processes, exhibit the same variation with pH as proton relaxation times and confirm the existence of a *bound water* fraction. The dispersion CPMG curves measured at 250 MHz for water relaxation rate are thus interpreted as due to an exchange contribution between water and exchangeable protons of soluble proteins or lactose.

NMR transverse relaxation times of water have been measured in skim-milk after renneting, which causes a gel network to be formed, and during the syneresis of the curd /10/. During the gelation process, transverse relaxation curves remain as single exponential and no change in water relaxation time is observed. Furthermore, the CPMG dispersion curve measured at high fields for skim-milk and renneted skim-milk remains very similar. As the exchange parameters obtained by the fitting procedure are not affected by the gelation process, it is likely that only exchangeable protons from soluble proteins and carbohydrates from whey are responsible for the dispersion curves. On the other hand, after syneresis, transverse relaxation curves must be analyzed in terms of two T_1 components – a short relaxation time component corresponding to water included in milk clot and

a long relaxation time component corresponding to whey expelled during syneresis. The multiexponentiality of the relaxation curves and the independence of T_2 values with the time of syneresis make it evident that diffusive exchange between the two types of water on the NMR timescale has a negligible effect, so that the percentages of the two components are directly related to the amount of water inside and outside the gel. In conclusion the quantitative interpretation of the ^1H relaxation curves can be used as a rapid and non-invasive method to monitor syneresis.

DIFFUSION MEASUREMENTS

Additional insight into the description of water mobility can be obtained by measuring the self-diffusion coefficient of water molecules. Unlike relaxation times, which are not simply related to water motional properties and whose interpretation is model dependent, experimental values of self-diffusion coefficients are easy to interpret, as they are directly related to the molecular displacement of water molecules in the laboratory frame. Furthermore, the interest in the study of diffusional processes in solution and in heterogeneous systems lies in the fact that diffusion data can provide information about the microstructure of the solid phase.

The pulsed field gradient NMR technique is a reliable method for determining molecular self-diffusion coefficients with good precision and relatively short measuring times /11/. The spin-echo experiment in the presence of an applied magnetic field gradient represents the basic method of NMR measurement of diffusion coefficients. The rationale of the approach stems from the following arguments: in the spin-echo experiment, nuclear spins, whose precession frequencies are kept constant during the experiment, are refocused at time 2τ, so that the precessing nuclear spins lose their phase coherence only as a result of the spin-spin relaxation mechanism (Fig. 1a). When a field gradient is present, nuclei in different positions in space are characterized by different precession frequencies. If nuclei undergo random and incoherent motion, such as Brownian motion, their precession frequencies will change correspondingly due to the different position in space with respect to the applied field gradient. This leads to an incomplete refocusing of spins at the echo time (Fig. 1b).

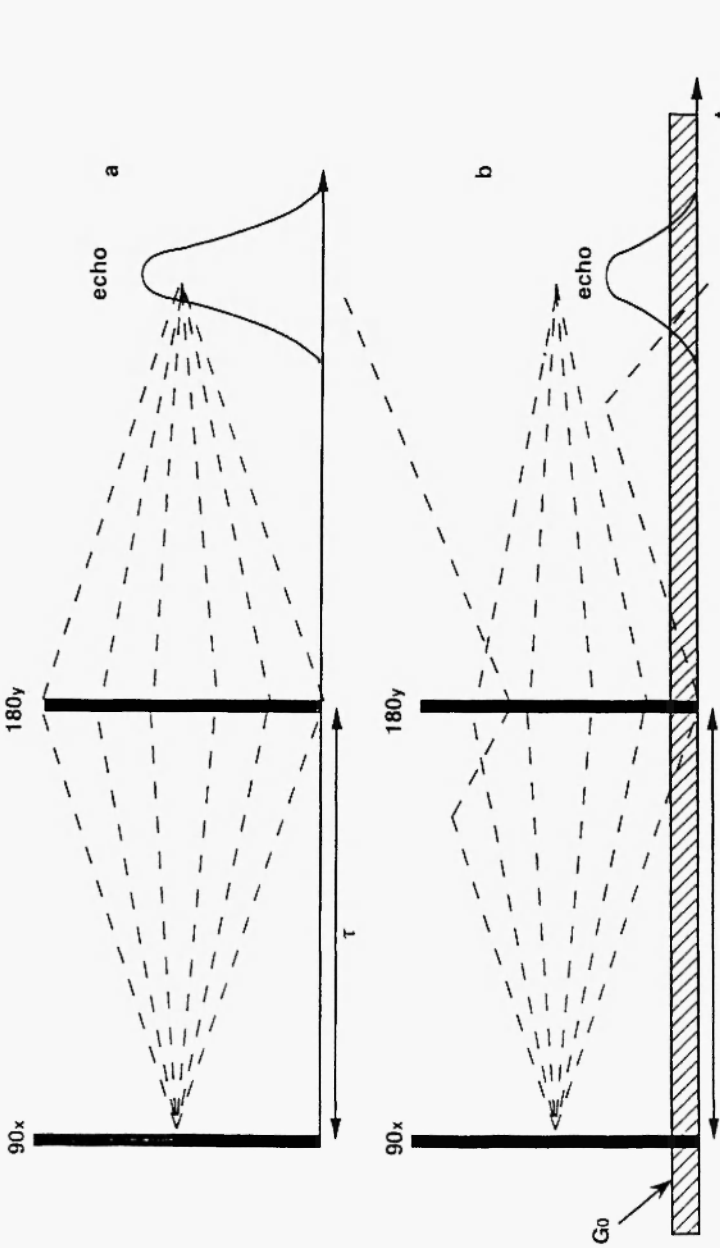

Fig.1. Evolution of nuclear phase angles during a spin-echo experiment in a homogeneous (a) and inhomogeneous (b) magnetic field. The echo attenuation depends on incomplete refocusing of spins undergoing incoherent motion.

Typically, a linear magnetic field gradient, $G_z=dB_0/dz$, is applied in a single direction. In earlier works steady gradients were used, while modern applications make use of pulsed field gradients, PFG.

The pulse sequence used in the PFG-SE experiment is shown in Fig. 2. Two gradient pulses, of amplitude G and duration δ, are applied. The first gradient pulse is applied before the 180 rf pulse, during the dephasing period, and labels the spins according to their position; the second gradient pulse is applied after the rf 180° pulse, during the rephasing period, and determines how far the spins have moved in the spacing between the two gradient pulses Δ.

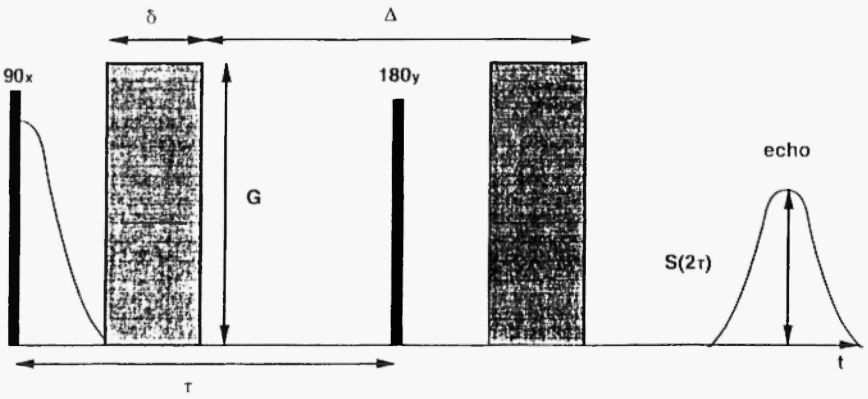

Fig.2. The Stejskal-Tanner PFG-SE sequence.

The amplitude S of the echo measured at time 2τ is a function of three independent variables: the strength of field gradient G, its duration δ, and the diffusion time Δ.

What is experimentally measured is the attenuation ratio R, defined as the ratio between the echo amplitude with gradient on and the echo amplitude with gradient off; R and the self-diffusion coefficient are related by the formula:

$$\ln R = -(\gamma\delta G)^2\left(\Delta - \frac{\delta}{3}\right)D$$

The slope of the straight line of a semilog plot of R vs $(\gamma\delta G)^2(\Delta-\delta/3)$ thus yields the diffusion coefficient D in the case of molecules undergoing random and unperturbed displacements, i.e. *free diffusion* (dotted line in Figure 3).

In heterogeneous systems, in which the existing physical barriers limit molecular translational motions during observation time, the net displacement becomes less than predicted by a gaussian diffusional process. This condition of *restricted diffusion* is evidenced by a deviation from a linear dependence of lnR vs $(\gamma\delta G)^2(\Delta-\delta/3)$ when Δ is increased (solid line in Fig. 3).

The pulsed field gradient technique was used to measure water and fat self-diffusion coefficients in *Cheddar* and *Swiss* cheese /12/. The echo attenuation plot for water protons measured at observation times up to 35 ms showed no deviation from linearity, giving a value of $D = (0.38 \pm 0.4)\cdot10^{-9}$ m^2s^{-1} for water in both types of cheese. From these data a minimum limit for diffusive domain size of $(6Dt)^{1/2} \sim 10$ μm has been obtained. The observed reduction of water diffusion coefficient value measured in cheese with respect to that of bulk water, $2.56\cdot10^{-9}$ m^2s^{-1}, can be accounted for both by the interaction of water molecules with protein surfaces and by local dimensionality. For the fat component, instead, the echo attenuation plot measured over a diffusion time of up to 180 ms showed an evident curvature typical of restricted diffusion. The initial slope of the measured plot gives a self-diffusion coefficient for fat of $\sim1.1\cdot10^{-11}$ m^2s^{-1}, about the same as for the bulk milk fat. By fitting the curvature of the measured attenuation plots and using an appropriate gaussian distribution of the sphere volumes, the mean radius, R_0, of the droplets can be obtained. The calculated standard deviation of fat sphere radii indicates a broad distribution of sizes. The values obtained for R_0, 2.1 μm and 2.6 μm for *Cheddar* and *Swiss* cheese, respectively, are lower than the root mean square displacement of 2.9 μm that fat molecules can undergo according to a self-diffusion coefficient of $\sim1.1\cdot10^{-11}$ m^2s^{-1}, confirming the evidence for restricted diffusion.

The diffusion coefficients for both water and fat in *Cheddar* and *Swiss* cheese can be separately measured, because signals for water and fat components are well resolved in the ^1H NMR spectrum.

Often food systems are characterized by several water-containing compartments that differ in relaxation times as well as in diffusion coefficients. Because of the identical chemical shifts and small differences among these diffusion coefficients, a single mean value for water mobility is generally

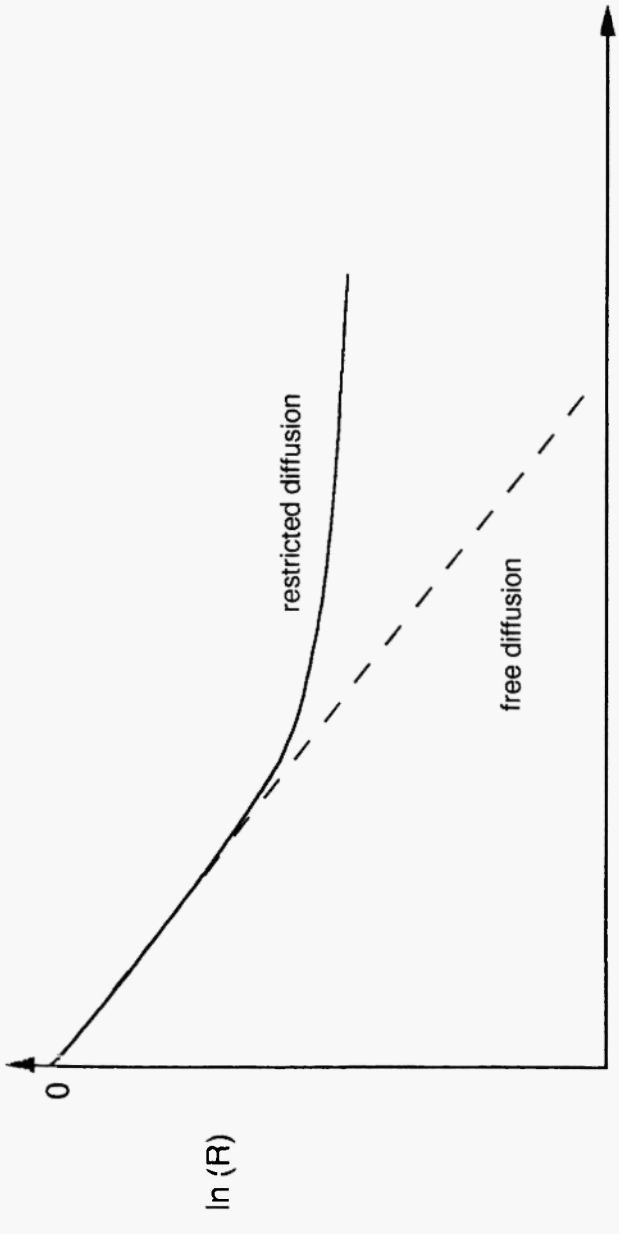

Fig.3. Dependence of ln(R) on $(\gamma G\delta)^2(\Delta-\delta/3)$ term for nuclear spins undergoing free (dashed line) and restricted (solid line) diffusion.

measured. A more accurate description of the system could be obtained by measuring the diffusion of molecules within different compartments. A recent paper /13/ demonstrated the possibility of measuring diffusion coefficients that are less than a factor of two apart, by combining CPMG T_2 measurements and diffusion measurements at various echo times. The method uses the analysis of a CPMG relaxation curve to determine the percentages of differing T_2 components and exploit the dependence of the apparent diffusion coefficient, D_{app}, on the echo time, TE, when measuring diffusion coefficient by the pulsed field gradient multiple spin echo technique (PFG MSE).

In this sequence (Fig. 4) two gradient pulses are superimposed on a modified CPMG pulse train. A careful choice of the number of π pulses before and between the gradients makes the independent selection of echo time and reduced diffusion time ($\Delta-\delta/w$) possible. Furthermore, setting an appropriate δ value, such that the condition $2/3\delta^2 \cong 2\tau^2$ is satisfied, allows the effects of *in situ* gradients arising from susceptibility differences within the sample to be eliminated.

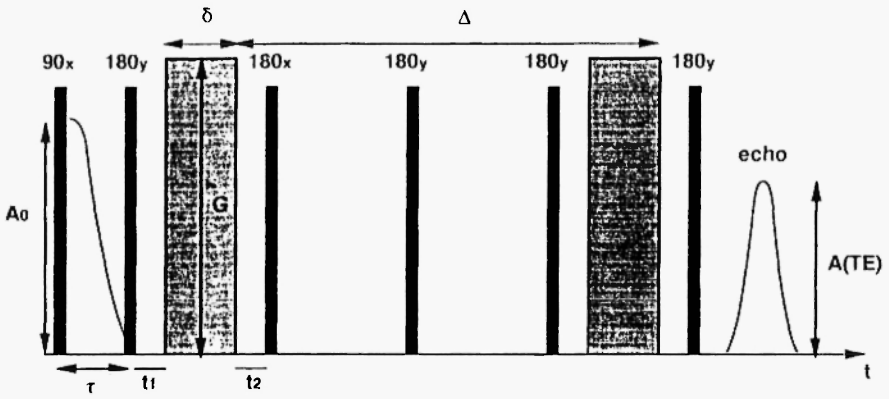

Fig.4. Representation of PFG-MSE sequence. Two gradient pulses are superimposed on a CPMG-like pulse train. Δ is varied by changing the number of π pulses between the gradients, according to the *xy*-8 phase scheme, the echo time (TE) by varying the total number of 180 pulses.

In a two-component system the actual D_i's can be calculated from the D_{app} value, as obtained by a monoexponential fit of R vs $(\gamma\delta G)^2(\Delta-\delta/3)$, using the following formula:

$$D_{app}(TE) = f_1(TE)D_1 + f_2(TE)D_2$$

where f_i(TE) is the signal amplitude fraction of component i at echo time TE, as determined by a biexponential fitting of a separate CPMG experiment with the same pulse spacing as MSE. Therefore, this method has been called *d*iffusion *a*nalysis by *r*elaxation *t*ime *s*eparated (DARTS) PFG-NMR.

By using this approach, the diffusion coefficient of water in the vacuole of apple parenchyma tissue ($D = 1.7\ 10^{-9}\ m^2s^{-1}$) was distinguished from that of the cytoplasm ($D = 1.0\ 10^{-9}\ m^2s^{-1}$) /13/. Here we report the preliminary results obtained using this new sequence on a *Ricotta* cheese sample measured at 25°C (Fig. 5). A biexponential fit of a CPMG curve, obtained at 2τ=2 ms on a Bruker Minispec PC120 low-resolution spectrometer equipped with a pulsed gradient unit, gave two water components, a more abundant component (88.3%) with a transverse relaxation time $T_2 = 42.2 \pm 0.3$ ms and a less abundant component (11.7%) with $T_2 = 179 \pm 4$ ms. The presence of a third component with an even lower relaxation time cannot be excluded, but in the following discussion will not be taken into consideration.

Taking into account the relative percentages of the two components, a tentative assignment was made, attributing the faster relaxing component to water molecules confined in caseine micelles and the other component to water outside the micelles.

MSE experiments at the same pulse rating were carried out at echo times of 18 and 150 ms, giving D_{app} values of $(0.84 \pm 0.001)\cdot10^{-9}\ m^2s^{-1}$ and $(0.64 \pm 0.08)\cdot10^{-9}\ m^2s^{-1}$, respectively ($\delta$= 1.732 ms, G = 0.6 ÷ 0.8 Tm^{-1}, Δ = 6 ms). The self-diffusion coefficients extracted by the previously described procedure are $D_1 = (0.5 \pm 0.2)\cdot10^{-9}\ m^2s^{-1}$ and $D_2 = (0.90 \pm 0.02)\cdot10^{-9}\ m^2s^{-1}$ for water outside and inside the casein micelles, indicating for both types of water a slower motion than that of pure water. Furthermore, it appears that molecules trapped inside the macromolecular network are characterized by a greater mobility than those assigned as "external". This difference could be explained in terms of a low-dimensional diffusive motion of a molecule when interacting with a surface.

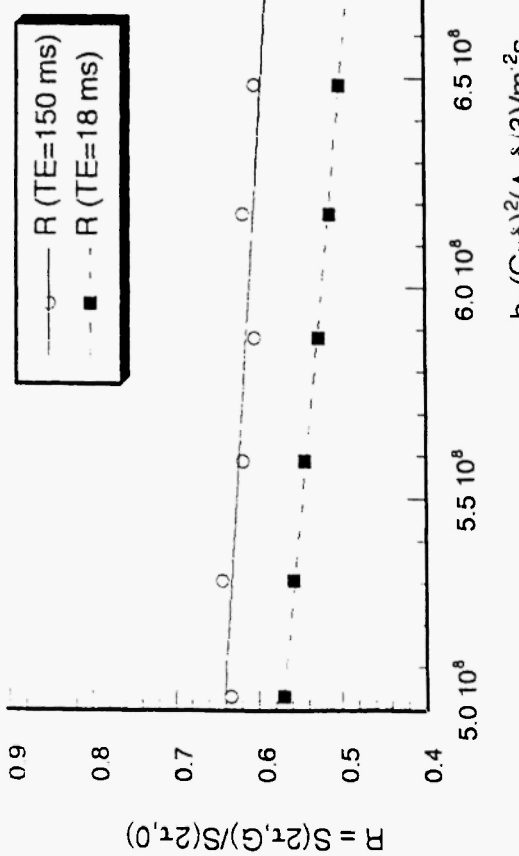

Fig.5. Plot of signal attenuation R versus $b=(G\gamma\delta)^2(\Delta-\delta/3)$ for water in a *Ricotta* cheese sample. Attenuation is measured with a PFG-MSE sequence at different echo times (TE=18 and 150 ms). Other parameters are Δ=6 ms, δ=1.732 ms, G=0.62-0.80 Tm^{-1}. Solid lines represent the monoexponential fit of the experimental points. The measurements were carried out on a Bruker Minispec PC120 low-resolution spectrometer.

HIGH-RESOLUTION SOLID-STATE NMR OF CHEESE

While it is relatively simple to use NMR to get information on the liquid components of food, in order to gain direct insight into solid components some problems must be overcome. The band width of signal from solids, in fact, has a size of at least 10 KHz and is practically undetectable. This is because of dipolar interactions between nuclei and chemical shift anisotropy. Both these effects are eliminated by spinning the sample at the so-called *magic angle*, ~54° 44′ (defined by the direction of magnetic field with probe axis), to simulate motional averaging. Residual dipolar interactions are removed by high power decoupling so that the Hartmann-Hahn condition is met. In this way magnetization is transferred from ^{1}H to ^{13}C nuclei, resulting in an increase in sensitivity. For this reason, although ^{1}H is the most abundant NMR nucleus, the dilute ^{13}C nuclei are the best choice for obtaining high resolution solid-state NMR spectra.

An example of the ^{13}C CPMAS spectrum of a sample of *Ricotta* cheese is reported in Fig. 6. The *Ricotta* cheese sample was purchased from a supermarket and preliminarily freeze-dried, in order to avoid phase separation while spinning in the probe.

Proton-decoupled ^{13}C NMR spectra were acquired using a Bruker AM400 spectrometer operating at 100 MHz for ^{13}C, equipped with a broad band MAS probe.

The ^{13}C CPMAS spectrum obtained for *Ricotta* cheese is very similar to that reported by Kakalis *et al.* /14/ for a *Cheddar* cheese sample.

Signals at δ=178 ppm, assigned to the carbonyl groups of the peptidic bond, were used as internal reference standard versus tetramethylsilane. The carbonyl signal is characterized by two intense side bands, arising from an incomplete averaging of the large chemical shift anisotropy of the carbonyl group. Signals between 15 and 40 ppm were assigned to side chain methylene and methyl groups, while resonances around 55 ppm corresponded to α-CH carbon atoms.

In addition to signals arising from a typical protein spectrum, peaks at 70-80 ppm and 90-105 ppm were observed. These signals were assigned to –CHOH and anomeric saccharide carbon atoms, respectively.

In any case the importance has to be underlined of resolving signals from α-CH, as the chemical shifts of these groups are very sensitive to the conformation of polypeptide chains. Furthermore, when different solid

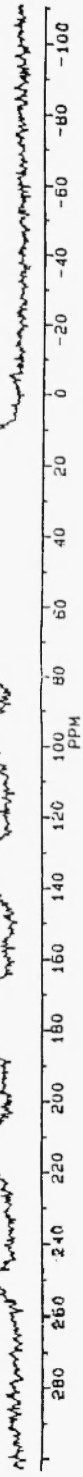

Fig.6. 100MHz CPMAS ^{13}C spectrum of a freeze-dried sample of *Ricotta* cheese (spectral parameters are: recycle delay = 2 s, spin-lock time = 1.2 ms, spectral width = 41667 Hz, time-domain size = 4 Kwords, spectral resolution = 10.2 Hz/pt). Labels indicate signal assignments (*ssb* denotes spinning side bands). We gratefully acknowledge the assistance of Prof. Maurizio Paci for recording this spectrum on his Bruker AM400 spectrometer (Università degli studi di Roma "Tor Vergata").

components are present in a sample, e.g. protein and lactose, the measurement of relaxation times of the resolved peaks in the CPMAS spectrum enables one to assess whether these components are intimately mixed or are in separate domains. It is our opinion that at the moment the ^{13}C CPMAS can only be used as a fingerprint of the protein component in cheese. Further work is necessary to improve the quality of the spectra, in order to ascertain differences among different types of cheese samples as well as to have the possibility of monitoring the influence of processing, ripening and storage on protein cheese structure.

HIGH-RESOLUTION NMR OF MILK

High-resolution NMR generally involves ^{1}H and ^{13}C nuclei. However, with the advent of high-field Fourier Transform NMR instruments many other nuclei can be measured. Of these, ^{31}P is widely used for the analysis of biological systems, because of the relatively high concentrations of phosphorus metabolites like ATP, phosphocreatine and inorganic phosphate that define the energy status of the cell.

The popularity of ^{31}P NMR is due to the fact that, although the sensitivity of ^{31}NMR is only 6% of that of ^{1}H NMR, ^{31}P NMR spectra cover a wide range of chemical shifts, and the resonance signals are relatively narrow and easily assignable to the limited number of phosphate compounds encountered in biological systems. Quantitative analysis of the different metabolites can thus easily be performed by measuring the areas under the resonance peaks /15/.

In the ^{31}P NMR spectrum of liquid whole or skim milk /16/ only three resonance signals are observed. Of these the most intense signal corresponds to inorganic phosphate, P_i, in solution; the other two peaks are assigned to seryl phosphate residues of casein and to a phosphate diester (probably glycerol-phosphoryl-choline). The signal from other phosphorus compounds cannot be observed because, in macromolecular aggregates such as casein micelles, the ^{31}P resonances are expected to be several kilohertz broad.

In the ^{31}P NMR spectrum of milk serum /17/ – measured at high pH values in order to avoid overlapping of some diester resonances – many other signals of phosphorus-containing molecules are observed and can be

assigned to glucose-6-phosphate, glycerol-1-phosphate, 3-phosphoglyceric acid, phosphorylethanolamine, phosphorylcholine, galactose-1-phosphate, lactose-1-phosphate, N-acetylglucosamine-1-phosphate, glycerophosphoryl-ethanolamine and phosphocreatine. The presence of the phosphocreatine signal at 2.32 ppm represents an unexpected result of this investigation because, while creatine and creatinine are known to be present in milk, the presence of phosphocreatine had previously not been reported in milk. Furthermore, some precursors of phospholipids have also been detected by analysis of the ^{31}P NMR spectrum, probably as a result of the enzymatic action of phospholipase on phospholipids or originating in leakage from the secretory cells. Thus, ^{31}P NMR seems to be a valuable and not completely exploited tool for the study of the phosphorus-containing compounds in milk.

CONCLUSIONS

Some examples of the use of different NMR techniques for the analysis of dairy products have been reported. Clearly, *high-resolution* NMR is the one that gives the most detailed information on the systems to be investigated, but it requires a preliminary sample preparation so that it is not generally used for the analysis of end products. The use of *solid state high-resolution* NMR and NMR *Imaging* /18/ is just starting and the potentiality of these techniques is not completely exploited.

Low-resolution NMR seems to be a valuable tool at present in the analysis of dairy products: it does not require any sample preparation, it is very simple and rapid, and it can be easily automated for routine and on-line controls.

REFERENCES

1. E. Brosio and A. Di Nola, *Trends in Analytical Chemistry,* **1**, 284 (1982).
2. S. Meiboom and D. Gill, *Rev. Sci. Instrum.*, 29, 688 (1957).
3. E. Brosio, G. Altobelli, S.Y. Yu and A. Di Nola, *J. Food Technol.*, **18**, 219 (1983).

4. E. Brosio, G. Altobelli and A. Di Nola, *J. Food Technol.*, **19**, 103 (1984).
5. B.P. Hills, C. Cano and P.S. Belton, *Macromolecules*, **24**, 2944 (1991).
6. B.P. Hills, S.F. Takacs and P.S. Belton, *Food Chem.*, **37**, 95 (1990).
7. P. Lambelet, R. Berrocal and F. Ducret, *J. Dairy Research*, **56**, 211 (1989).
8. S.P.F.M. Roefs, H. Van As and T. Van Vliet, *J. Food Science*, **54**, 704 (1989).
9. F. Mariette, C. Tellier, G. Brulé and P. Marchal, *J. Dairy Research*, **60**, 175 (1993).
10. C. Tellier, F. Mariette, J.P. Guillement and P. Marchal, *J. Agric. Food Chem.*, **41**, 2259 (1993).
11. O.S. Stejskal and J.E. Tanner, *J. Chem. Phys.*, **42**, 288 (1965).
12. P.T. Callaghan, K.W. Jolley and R.S. Humphrey, *J. Colloid Interface Sci.*, **93**, 521 (1983).
13. D. Van Dusschoten, P.A. De Jager and H. Van As, *J. Magnet. Reson., Ser. B*, **116**, 22 (1995).
14. L.T. Kakalis, T.F. Kunosinski and H.M. Farrell Jr., *J. Dairy Sci.*, 77, 667 (1993).
15. D.I. Hoult, S.J.W. Busby, D.G. Gadian, G.K. Radda, R.E. Richards and P.J. Seeley, *Nature*, **252**, 285 (1974).
16. P.S. Belton, R.L.J. Lyster and C.P. Richards, *J. Dairy Research*, **52**, 47 (1985).
17. M. Wahlgren, T. Drakenberg, H.J. Vogel and P. Dejmek, *J. Dairy Research*, **53**, 539 (1986).
18. M. Rosemberg, M. McCarthy and R. Kanten, *J. Dairy Sci.*, **75**, 2083 (1991).